



PII S0016-7037(96)00230-X

## A 200 year mid-European air temperature record preserved in lake sediments: An extension of the $\delta^{18}\text{O}_p$ -air temperature relation into the past

ULRICH VON GRAFENSTEIN,<sup>1,\*</sup> HELMUT ERLKENKEUSER,<sup>2</sup> JENS MÜLLER,<sup>1</sup> PETER TRIMBORN,<sup>3</sup> and JOACHIM ALEFS<sup>1</sup>

<sup>1</sup>Lehrstuhl für Allgemeine, Angewandte und Ingenieur-Geologie, Technische Universität München, D-85747 Garching, Germany

<sup>2</sup>C14-Labor des Instituts für Reine und Angewandte Kernphysik, Christian-Albrecht-Universität Kiel, D-24098 Kiel, Germany

<sup>3</sup>GSF-Institut für Hydrologie, Neuherberg, Postfach 1129, D-85758 Oberschleißheim, Germany

(Received December 13, 1995; accepted in revised form June 28, 1996)

**Abstract**—A detailed history of the water oxygen isotope ratios of Lake Ammersee, southern Germany, was established for the last two centuries by analyzing oxygen isotope ratios of ostracod shells from a sediment core in a three- to five-year resolution. Empirical analysis and modelling of the isotope hydrology of the lake show that the oxygen isotopic composition of the lake water is mainly controlled by the isotopic composition of local precipitation. For the last 200 years, the lake isotope record is strongly correlated to the air temperature record from Hohenpeißenberg, situated within the lake's catchment area. Thus, the mid-European relation between  $^{18}\text{O}$  in precipitation and air temperature, documented for the last 20 years, can be extended over a longer time and a larger temperature range. The results provide further support for the validity of ostracod  $\delta^{18}\text{O}$  from Ammersee sediments as a quantitative proxy for mean annual air temperature, probably extending back to the last glaciation.

### 1. INTRODUCTION

The temporal  $\delta^{18}\text{O}_p$ -temperature relation is the foundation of many attempts to reconstruct paleotemperatures, yet it has never been thoroughly evaluated beyond the limited range of direct precipitation sampling and instrumental temperature documentation. Dansgaard (1964) showed that the spatial distribution of mean annual air temperature and weighted mean annual  $\delta^{18}\text{O}$  of precipitation ( $\delta^{18}\text{O}_p$ ) for the northern hemispheric coastal stations are strongly correlated. Rozanski et al. (1992) empirically derived a relation between air temperatures and  $\delta^{18}\text{O}_p$  for temporal changes from datasets from several locations spanning the past 30 years. The data show a rather strong correlation between both yearly and monthly means of temperature and the isotopic composition of precipitation in central and western Europe, but the slopes of these linear correlations vary considerably for the individual sites. Moreover, mean annual air temperature variations during the last 30 years only cover a small range of about 2°C. It remained unproven, therefore, whether the  $\delta^{18}\text{O}_p$ -temperature relation holds true over a longer period of time and a larger range of temperature variations. Jouzel et al. (1994) compared temperatures and  $\delta^{18}\text{O}_p$  from general circulation model (GCM) runs simulating modern and glacial conditions. According to their study the spatial  $\delta^{18}\text{O}_p$ -temperature relation of the last 30 years in Europe also held for the last glacial maximum. Stute (1989) found a similar  $\delta^{18}\text{O}_p$ -temperature relationship by comparing late glacial and modern  $\delta^{18}\text{O}$  of Hungarian groundwaters with air temperature derived from noble gas contents, as did Rozanski (1985) for groundwater  $\delta^{18}\text{O}$  and air temperatures derived from GCMs.

Polar ice cores preserve original precipitation and its isotopic history over the last 300 kY in a subyearly resolution

(e.g., Johnsen et al., 1992). Due to the lack of long instrumental temperature records, however, even this ideal paleoclimatic archive remained essentially uncalibrated. Recently, bore hole temperature profiles measured at Summit (Greenland) were compared with temperature profiles calculated from the isotope record for the GISP2 (Cuffey et al., 1995) and GRIP (Johnsen et al., 1995) ice cores, using varying temporal  $\delta^{18}\text{O}$ -temperature coefficients. Independently, both studies achieve the best fit of modelled and measured ice temperatures with  $\sim 0.33\%/^{\circ}\text{C}$  and, therefore, conclude much lower temperatures for the last glacial maximum than assumed before.

In temperate humid areas, the isotopic composition of precipitation may be derived from material formed in isotopic equilibrium with groundwater such as cave deposits or from more indirect archives of  $\delta^{18}\text{O}_p$  in other aquatic and terrestrial deposits. However, the value of continental oxygen isotope records as paleoclimatic proxies and especially their transformation into conventional climatic parameters such as mean annual air temperature (MAAT) depends on the robustness of the local relation between surface air temperature and  $\delta^{18}\text{O}_p$  and, in addition, on the linkage between  $\delta^{18}\text{O}_p$  and  $\delta^{18}\text{O}$  of the water from which the archive was formed. We analyzed a highly resolved record of  $\delta^{18}\text{O}$ -variations of ostracod shells from a sediment core from Lake Ammersee (Bavaria) and compared this record with air temperatures measured for the last 200 years at Hohenpeißenberg, a meteorological observatory within the catchment area of the lake. The study provides evidence that a simple linear relation between  $\delta^{18}\text{O}_p$  and MAAT may be valid for this entire period, including parts of the Little Ice Age, and hence over a larger range of temperature variation than that of the last 30 years. Additionally, this study provides a direct test of the reliability of oxygen isotope records from the lake's sediments, including possible alterations of the  $\delta^{18}\text{O}$ -signal on its way from the precipitation to the final preservation in

\* Present address: Laboratoire de Modelisation du Climat et de l'Environnement, LCME, CEA/DSM CE Saclay, 91191 Gif-Sur-Yvette, France.

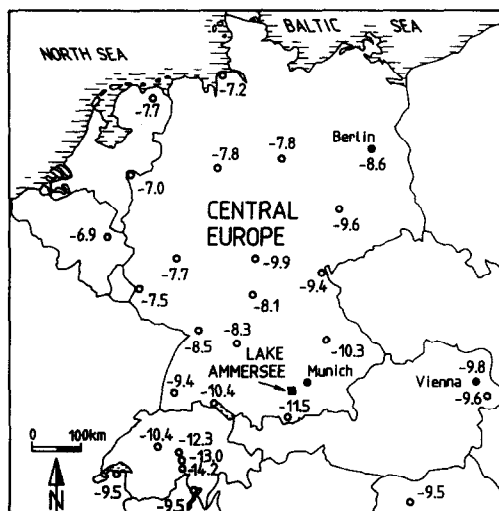


FIG. 1. Map showing the distribution of long-term arithmetic mean  $\delta^{18}\text{O}_p$  at IAEA/WMO stations in central Europe (modified after McKenzie and Hollander, 1993). Data are from Rozanski et al. (1993), stations are indicated by circles, the location of Ammersee is shown by the filled square.

ostracod shells. Records of  $\delta^{18}\text{O}$  in precipitation at Hohenpeißenberg covering the last 20 years, together with a four-year investigation of stable isotope ratios in lake water samples, gives further evidence that the oxygen isotope composition of Lake Ammersee ( $\delta^{18}\text{O}_L$ ) is highly sensitive to changing mean annual air temperatures.

## 2. MATERIAL AND METHODS

In 1988 a short gravity core (AS Tmax 88) of 116 cm length was taken in the central part of Lake Ammersee (see Fig. 1 for location) in 80 m water depth. The lake bottom for at least 1 km<sup>2</sup> around the core site is flat and shows no evidence of slides or other disruptions. According to surveys in 1992–1994, Lake Ammersee is monomictic. At least 80% of its recharge comes from the river Ammer, which drains a catchment extending ca. 50 km to the south and including parts of the northern Alps. The mean theoretical residence time of Lake Ammersee water, as expressed by the ratio of input to volume is 2.7 years (Grimminger, 1982). The only significant human alteration of the hydrological balance occurred in 1922, when the Ammer was canalized, the inflow was repositioned, and an extended wetland downstream was drained (Grimminger, 1982). These measures were intended to accelerate the passage of flood runoff through the system.

### 2.1. Core Chronology

Chronological and microstratigraphic studies were carried out on a core (AS Tmax 93) taken at the same site as AS Tmax 88 in 1993. Alefs et al. (1996) could demonstrate the annual character of light-dark lamina accompanied by seasonal diatom successions back to 1958. Light layers represent summer calcite precipitation separated by coarser material from the littoral zone, redeposited during the turnover period in fall and winter. Before 1958, the diatom cell numbers in the thin sections decrease significantly. Therefore, the annual nature of the light-dark lamina can only be assumed because the characteristics (calclitic layers separated by littoral debris) remain essentially unchanged throughout the core. Additional chronological control is given by the fact that, based on layer counting, ages of prominent homogenous layers of detrital material match with historically documented flood events. The chronology established for core AS Tmax 1993 had to be transferred to core AS Tmax 88, which had been completely used up for sedimentological and

geochemical analysis. Marker beds clearly identified on core photographs from both cores were used to provide fixed ages (Fig. 2). Ages in between these marker beds are from counting layers, if calcitic layers were visible on the photograph of core AS Tmax 88, or from linear interpolation between the marker beds.

For the uppermost part, these varve-based ages attributed to core AS Tmax 88 are consistent with ages derived from <sup>137</sup>Cs- and <sup>134</sup>Cs-measurements on AS Tmax 88 (J. Müller et al., unpubl. data). The final precision of the core chronology of AS Tmax 88 is controlled by the errors of varve counting in core AS Tmax 93, where years might be missing or added due to counting of pale homogenous layers not representing an annual cycle. In addition, errors might be introduced by the core to core correlation.

Based on our age model, a single 1-cm sample represents an average time of 2.85 years. The existence of distinct calcitic layers throughout the cores at least gives evidence that bioturbational mixing should be minor.

### 2.2. Oxygen Isotope Record of Ostracods

Ostracod and mollusc shells were separated from samples of ca. 15 cm<sup>3</sup> taken continuously every centimeter throughout the core.

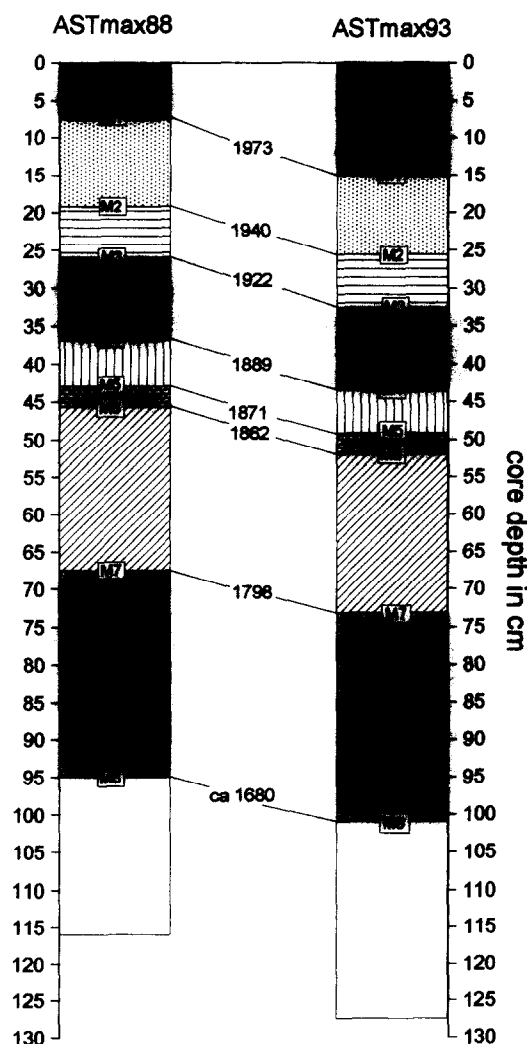


FIG. 2. Marker layers identifiable in both core AS Tmax 93 (dated by varve counting in thin sections) and core AS Tmax 88 (used for stable isotope analysis). The marker bed ages were used as fixed points in the depth-age model for AS Tmax 88, ages in between these marker beds are by interpolation or layer counting on a core photograph.

The samples were disaggregated in a 10% hydrogen peroxide solution and washed through a 125  $\mu\text{m}$  sieve. The coarse fraction was rinsed in ethanol after sieving to avoid contamination with dissolved carbonate in tap water. The valves in the samples represent only benthic species common to deep lake conditions (*Candona lozeki*, *C. levanderi*, *C. candida*, *Cytherissa lacustris*, *Ilyocypris bradyi*, *Leucocythere mirabilis*). No shells of species restricted to the littoral zones of Lake Ammersee were found. We, therefore, believe that the shell material represents the in situ fauna. For stable isotope measurements at least two sets of 20–30 shells of juvenile *C. levanderi* and *C. candida* (instars 5–8) were picked from a sample and, if necessary, were cleaned with paint brush and ethanol. The abundance of adult carapaces, ranging from zero to ten per sample and species, was too low to produce a continuous and significant isotopic record. The stable-isotope composition of the shell material was analyzed on the automatic CARBO Kiel/MAT 251  $\text{CO}_2$ -preparation and mass-spectrometer system at CAU Kiel. Isotope ratios of the shells are given relative to the PDB Standard in the conventional  $\delta$ -notation, with analytical uncertainties of  $\pm 0.05\text{‰}$  and  $\pm 0.08\text{‰}$  for  $\delta^{13}\text{C}$  and  $\delta^{18}\text{O}$ , respectively.

According to observations of the living faunas in the sample area (1992 through 1994), calcification of the small instars used for the isotope record takes place during the winter season. The shells should therefore represent mixing conditions, when  $\delta^{18}\text{O}$  of the water is uniform throughout the water column. Water temperature at 80 m depth is  $4 \pm 1.0^\circ\text{C}$  throughout the year and varies over an even narrower range in winter. In the uppermost 9 cm of the core no shells of benthic calcite-producing organisms were present, apparently because of oxygen depletion in the bottom waters. *Candona* became reestablished in abundance around 1990 and shells of living ostracods collected from 1992–1994 were analyzed for their stable isotope ratios to describe present-day conditions. Mean  $\delta^{18}\text{O}_{\text{C.s.}}$  of replicates from 15 individuals (instars 6 and 7) is  $-4.60\text{‰}$  for the winter 1992–1993 ( $\delta^{18}\text{O}_{\text{L}} = -9.59\text{‰}$ ) and  $-4.68\text{‰}$  for the winter 1993–1994 ( $\delta^{18}\text{O}_{\text{L}} = -9.50$ , Table 1). Actual  $\delta^{18}\text{O}_{\text{C.s.}}$  in both seasons is enriched compared to the isotopic composition of a theoretical calcite formed isotopic equilibrium ( $\delta^{18}\text{O}_{\text{eq}}$ ). The difference is  $+2.3 \pm 0.1\text{‰}$  to a  $\delta^{18}\text{O}_{\text{eq}}$  calculated using the fractionation factors given by Friedman and O'Neil (1977) and exactly matches the vital offsets for adults and juveniles of these species found during a one-year calibration study in Ammersee and Starnberger See, which will be presented and discussed elsewhere.

### 2.3. Stable Isotope Composition of Precipitation, Runoff, and Lake Water

$\delta^{18}\text{O}$  and  $\delta\text{D}$  of precipitation at Hohenpeißenberg has been monitored since 1973 as part of a worldwide network (IAEA, Rozanski et al., 1992). Weighted monthly samples are produced by mixing of daily precipitation samples proportional to the amount of the daily precipitation. Lake Ammersee water was collected for isotope measurements every two weeks from 0, 6, 12, 16, and 20 m water depth from September 1989 to December 1990. Water samples were also taken throughout 1992–1994 at 14 day intervals from different water depths (0, 1, 5, 10, 20, and 78 m) above the core position, from the main tributary Ammer, and from the outflowing river Amper. Daily samples of the river Ammer water, derived from aliquots taken every 20 min, were obtained for the period January 1993 to July 1994. Mean daily discharge of the river Ammer is continuously monitored by the Wasserwirtschaftsamt Weilheim. Oxygen and hydrogen isotope ratios were measured at GSF-Neuherberg according to the guidelines of the IAEA network (Rozanski et al., 1992) and are expressed in terms of  $\delta$ -values relative to the V-SMOW (Vienna Standard Mean Ocean Water) standard. The measurements are accurate within  $1\text{‰}$  for  $\delta\text{D}$  and  $0.15\text{‰}$  for  $\delta^{18}\text{O}$ .

### 2.4. Climate Data 1783–1994

Air temperatures have been measured since 1783 at Hohenpeißenberg, a meteorological station within the catchment of Lake Ammersee. Mean monthly air temperatures for the period 1783–1980 were provided by the German Meteorological Service

(Deutscher Wetterdienst), and extracted from monthly reports (Deutscher Wetterdienst, 1981–1994) for January 1981 to July 1994. Mean temperatures were calculated as arithmetic means of monthly temperatures for calendar years. Schönwiese (1987) demonstrated that the record is robust and free of interference due to urbanization or changes in instrumentation or position. He also established the existence of the quasi-biennial ENSO-cycle and a 10- to 13-year cycle attributed to sunspot activity in the record. Monthly precipitation data are available for the period 1880–1994.

## 3. RESULTS

### 3.1. Isotopic Composition of Precipitation and Air Temperatures (1973–1992)

The nineteen-year record of stable isotopic composition of precipitation demonstrates a strong dependency on both monthly and annual air temperatures although the slopes vary because precipitation is not equally distributed over the year. The most convincing demonstration of this dependency is obtained from comparison of three-year running means of  $\delta^{18}\text{O}_{\text{P}}$  (weighted by precipitation amount) and MAAT (Fig. 3), which clearly shows the isotopic expression of stepwise warmings from 1980–1983 and from 1986–1993, with a slope coefficient of about  $1.25\text{‰}/^\circ\text{C}$ . As noted below, smoothing of the records over a three-year window is also believed to closely approximate the expected isotopic response of the Ammer river to seasonally and annually changing  $\delta^{18}\text{O}_{\text{P}}$ , because of the natural attenuation of signals due to mixing and varying retention times as water passes through the catchment.

### 3.2. Isotopic Composition of River and Lake Water

$\delta^{18}\text{O}$ -values in samples from the river Ammer ( $\delta^{18}\text{O}_{\text{Am}}$ , Fig. 4b) display seasonal changes, although these are much smaller than the seasonal variations in  $\delta^{18}\text{O}_{\text{P}}$ . Under conditions of moderate to low runoff the Ammer only deviates by about  $\pm 0.5\text{‰}$  from the mean  $\delta^{18}\text{O}_{\text{P}}$  of the last three years. During times of higher runoff (Fig. 4a), the signal becomes more variable, showing spikes to higher  $\delta^{18}\text{O}$  values during the warm seasons and to lower values during colder seasons, corresponding with heavy rains or snow melt. The highest deviation from the mean occurred in April 1994, when after heavy rainfall the  $\delta^{18}\text{O}$ -values in the river Ammer dropped by over  $4\text{‰}$  within one day causing a temporal  $0.2\text{‰}$  decrease in the epilimnion. Evidently, the river Ammer is effectively transferring both low and high frequency fluctuations in  $\delta^{18}\text{O}_{\text{P}}$  to the lake.

The  $\delta^{18}\text{O}$  data obtained from different water depths in Lake Ammersee from 1990 through 1994 clearly document the cycle of seasonal stratification and mixing of the water column. During warm seasons, the epilimnion is enriched by up to  $0.8\text{‰}$  compared to the hypolimnion. This intra-lake difference is partly caused by evaporation, which only directly affects the epilimnion, and partly by the higher  $\delta^{18}\text{O}$  of summer inflow during times of high precipitation, which is preferentially added to the epilimnion because of thermal stratification. This seasonal effect is apparent from records of surface and bottom water  $\delta^{18}\text{O}$  (Fig. 4c). Water from the epilimnion is selectively lost to outflow during stratification,

TABLE 1.  $\delta^{18}\text{O}$  and  $\delta^{13}\text{C}$  of *Candona* sp. (juveniles) from core AS Tmax 88, Ammersee, 80 m water depth (see also Fig. 1).  $\delta^{18}\text{O}_m$  and  $\delta^{13}\text{C}_m$  give the arithmetic mean,  $\delta^{18}\text{O}_w$  and  $\delta^{13}\text{C}_w$  the average weighted by the number of carapaces per individual sample. Ages are from counting light-dark couplets in a parallel core. Corr. gives the correction of these ages which we had to introduce to achieve best fit to the air temperature history.

Depth	Age AD	Corr.	$\delta^{18}\text{O}$ individual values				$\delta^{18}\text{O}_m$	$\delta^{18}\text{O}_w$	$\delta^{13}\text{C}$ individual values				$\delta^{13}\text{C}_m$	$\delta^{13}\text{C}_w$
living	1993,0		-4,61	-4,59			-4,60	-4,60	-10,93	-10,42			-10,66	-10,66
living	1994,0		-4,67	-4,72	-4,64	-4,63	-4,67	-4,68	-10,42	-10,28	-9,52	-9,58	-9,95	-10,08
9,5	1986,6		-5,37				-5,37	-5,37	-9,94				-9,94	-9,94
11,5	1984,3		-4,70				-4,70	-4,70	-10,17				-10,17	-10,17
12,5	1982,1		-4,84				-4,84	-4,84	-9,78				-9,78	-9,78
13,5	1989,6		-4,77				-4,77	-4,77	-9,88				-9,88	-9,88
14,5	1986,9		-4,73				-4,73	-4,73	-9,42				-9,42	-9,42
15,5	1983,4		-4,62				-4,62	-4,62	-9,47				-9,47	-9,47
16,5	1949,7		-5,05	-4,83	-4,90	-5,24	-5,01	-5,11	-9,68	-9,37	-9,48	-9,84	-9,59	-9,71
17,5	1946,5		-5,22	-5,31	-5,12		-5,22	-5,23	-9,49	-10,00	-9,73		-9,74	-9,74
18,5	1943,9		-5,29				-5,29	-5,29	-10,25				-10,25	-10,25
19,5	1941,8		-5,03				-5,03	-5,03	-9,29				-9,29	-9,29
20,5	1939,0	1	-4,90	-5,01			-4,96	-5,01	-9,02	-9,31			-9,17	-9,30
21,5	1936,0	4	-4,77				-4,77	-4,77	-9,06				-9,06	-9,06
22,5	1932,4	8	-4,82	-4,79			-4,81	-4,81	-8,78	-8,91			-8,85	-8,85
23,5	1929,6	8	-4,96				-4,96	-4,96	-8,90				-8,90	-8,90
24,5	1927,7	9	-5,07	-4,97			-5,02	-5,03	-8,79	-9,22			-9,01	-8,98
25,5	1925,8	10	-4,85				-4,85	-4,85	-10,11				-10,11	-10,11
26,5	1922,4	11	-4,76	-4,88			-4,82	-4,83	-8,46	-8,89			-8,67	-8,70
27,5	1919,0	11	-4,82	-5,17			-5,00	-5,00	-9,25	-8,97			-9,11	-9,11
28,5	1915,9	11	-4,91	-4,73			-4,82	-4,83	-9,26	-8,93			-9,10	-9,11
29,5	1912,2	11	-4,76	-5,02			-4,89	-4,93	-9,27	-9,39			-9,33	-9,35
30,5	1908,9	11	-4,82	-4,94			-4,88	-4,90	-9,58	-9,14			-9,36	-9,29
31,5	1906,2	11	-4,78	-4,69			-4,74	-4,72	-9,45	-9,28			-9,37	-9,34
32,5	1903,3	11	-4,82	-4,88			-4,85	-4,85	-9,69	-9,30			-9,50	-9,50
33,5	1899,9	11	-4,87	-4,93			-4,90	-4,91	-8,62	-9,06			-8,85	-8,93
34,5	1896,4	11	-4,76	-4,60			-4,66	-4,65	-8,49	-8,72			-8,61	-8,64
35,5	1893,7	11	-4,75	-4,44			-4,60	-4,52	-8,99	-8,78			-8,89	-8,84
36,5	1891,7	11	-4,78	-5,03			-4,90	-4,92	-8,79	-9,39			-9,09	-9,13
37,5	1889,2	11	-5,20	-5,04			-5,12	-5,11	-9,28	-9,52			-9,40	-9,42
38,5	1886,1	11	-5,17	-5,15			-5,16	-5,16	-8,83	-9,36			-9,10	-9,07
39,5	1882,8	11	-4,93	-5,11			-5,02	-5,07	-8,49	-9,10			-8,80	-8,98
40,5	1879,5	11	-4,88	-5,23			-5,06	-5,17	-9,51	-8,93			-9,22	-9,03
41,5	1876,3	11	-5,03	-5,10			-5,07	-5,08	-9,29	-9,14			-9,21	-9,18
42,5	1873,6	11	-4,51	-5,02			-4,76	-4,85	-9,09	-8,61			-8,85	-8,77
43,5	1871,1	11	-4,74	-4,88			-4,81	-4,81	-9,70	-9,52			-9,61	-9,61
44,5	1868,2	11	-5,59	-4,85			-5,22	-4,97	-9,23	-9,25			-9,24	-9,25
45,5	1864,8	11	-4,60	-5,18			-5,04	-5,10	-9,54	-8,86			-9,20	-9,05
46,5	1861,9	8	-4,66	-4,83			-4,75	-4,77	-8,67	-9,03			-8,85	-8,91
47,5	1858,9	6	-4,93	-4,96			-4,94	-4,95	-8,93	-9,35			-9,14	-9,21
48,5	1856,6	4	-4,95	-4,99			-4,97	-4,98	-9,44	-9,41			-9,43	-9,42
49,5	1853,6	2	-5,26	-5,06			-5,16	-5,13	-9,13	-9,00			-9,07	-9,04
50,5	1850,0		-5,36	-5,27			-5,32	-5,32	-9,40	-9,61			-9,51	-9,49
51,5	1847,0		-5,00				-5,00	-5,00	-9,19				-9,19	-9,19
52,5	1843,4		-4,60	-5,01			-4,81	-4,90	-8,98	-8,78			-8,88	-8,83
53,5	1838,7		-4,72	-4,62			-4,67	-4,65	-8,54	-9,10			-8,82	-8,85
54,5	1834,3		-5,05	-5,02			-5,04	-5,03	-9,15	-8,99			-9,07	-9,04
55,5	1829,8		-5,07	-4,96			-5,01	-5,00	-9,17	-8,72			-8,95	-8,87
56,5	1826,9		-4,79	-4,75			-4,77	-4,76	-8,99	-9,05			-9,02	-9,03
57,5	1824,4		-4,70	-4,87			-4,79	-4,79	-9,10	-9,52			-9,31	-9,31
58,5	1821,9		-5,26	-5,08			-5,18	-5,15	-8,54	-8,90			-8,72	-8,77
59,5	1819,1		-4,99	-4,94			-4,97	-4,96	-8,56	-8,97			-8,76	-8,78
60,5	1816,1		-4,88	-4,68			-4,78	-4,75	-10,40	-9,60			-10,00	-9,90
61,5	1813,6		-4,79	-4,35			-4,57	-4,63	-8,85	-9,53			-9,19	-9,10
62,5	1811,5		-4,86	-4,90			-4,86	-4,86	-9,03	-8,88			-8,96	-8,96
63,5	1809,4		-4,86	-4,77			-4,82	-4,79	-8,83	-8,88			-8,86	-8,87
64,5	1807,2		-4,86	-4,84			-4,85	-4,85	-8,88	-8,82			-8,85	-8,84

TABLE 1. (Continued)

Depth	Age AD	Corr	$\delta^{18}\text{O}$ individual values			$\delta^{18}\text{O}$ m	$\delta^{18}\text{O}$ w	$\delta^{13}\text{C}$ individual values			$\delta^{13}\text{C}$ m	$\delta^{13}\text{C}$ w
65.5	1804.5		-5.03	-4.80		-4.92	-4.86	-9.70	-8.67		-8.66	-8.66
66.5	1801.7		-4.89			-4.89	-4.89	-9.74			-9.74	-9.74
67.5	1799.4		-4.77	-4.71		-4.74	-4.72	-8.82	-8.95		-8.99	-8.94
68.5	1797.9		-4.67	-4.79		-4.73	-4.75	-9.26	-8.94		-9.10	-9.04
69.5	1796.4		-4.44	-4.53		-4.49	-4.49	-8.85	-9.02		-8.94	-8.95
70.5	1794.0		-4.20	-4.50		-4.35	-4.43	-8.42	-9.05		-8.74	-8.90
71.5	1791.7		-4.46	-4.54		-4.50	-4.53	-8.84	-8.95		-8.90	-8.93
72.5	1789.4		-4.63	-5.32		-4.97	-5.07	-8.75	-9.21		-8.98	-9.04
73.5	1787.1		-4.82	-5.36		-5.09	-5.22	-9.28	-9.14		-9.21	-9.18
74.5	1784.8		-4.96	-5.52		-5.24	-5.37	-8.53	-8.95		-8.74	-8.84
75.5	1782.5		-4.82	-4.91		-4.87	-4.90	-9.22	-9.09		-9.15	-9.10
76.5	1780.2		-4.64	-4.86		-4.75	-4.83	-9.99	-9.34		-9.67	-9.43
77.5			-4.46	-4.43	-4.52	-4.46	-4.50	-8.67	-8.78	-8.66	-8.70	-8.69
78.5			-4.45	-4.54		-4.50	-4.53	-8.44	-8.90		-8.67	-8.66
79.5			-4.65	-4.70		-4.68	-4.69	-8.84	-9.02		-8.83	-8.92
80.5			-4.45	-4.44	-4.44	-4.44	-4.44	-9.63	-8.72	-8.79	-9.05	-8.82
81.5			-4.73	-4.74		-4.74	-4.74	-8.80	-8.84		-8.82	-8.83
82.5			-4.71	-4.65		-4.68	-4.67	-8.75	-9.10		-8.93	-9.00
83.5			-4.73	-4.76		-4.75	-4.75	-8.90	-8.92		-8.91	-8.91
84.5			-4.80	-4.79		-4.80	-4.79	-8.13	-8.40		-8.26	-8.33
85.5			-5.05	-5.13		-5.09	-5.10	-8.82	-8.91		-8.87	-8.86
86.5			-4.84	-5.00		-4.92	-4.95	-8.50	-9.12		-8.81	-8.91
87.5			-4.57	-4.73		-4.65	-4.67	-8.62	-8.57		-8.60	-8.59
88.5			-4.75	-4.70		-4.72	-4.71	-8.79	-8.87		-8.83	-8.85
89.5			-5.05	-4.93		-4.99	-4.96	-8.58	-8.70		-8.64	-8.67
90.5			-5.08	-5.05		-5.07	-5.06	-9.24	-9.32		-9.28	-9.29
91.5			-4.98	-5.04		-5.01	-5.02	-8.85	-9.24		-9.05	-9.08
92.5			-5.12	-5.25		-5.19	-5.19	-8.72	-8.96		-8.84	-8.86
93.5			-5.29	-5.03		-5.16	-5.12	-9.46	-9.20		-9.34	-9.29
94.5			-4.96	-4.73		-4.85	-4.76	-9.14	-9.18		-9.16	-9.17
95.5			-4.46	-4.47		-4.46	-4.47	-8.70	-8.79		-8.74	-8.76
96.5			-4.64	-4.49		-4.57	-4.54	-8.69	-8.84		-8.76	-8.79
97.5			-4.66	-4.80		-4.84	-4.83	-8.66	-8.83		-8.75	-8.77
98.5			-4.81	-4.84		-4.82	-4.83	-9.23	-8.81		-9.02	-8.96
99.5			-4.94	-4.90		-4.92	-4.92	-9.07	-8.81		-8.94	-8.91
100.5			-4.91			-4.91	-4.91	-8.73			-8.73	-8.73
101.5			-4.88			-4.88	-4.88	-8.92			-8.92	-8.92
102.5			-5.11	-5.43		-5.27	-5.36	-9.10	-9.46		-9.29	-9.39
103.5			-4.50			-4.50	-4.50	-8.86			-8.86	-8.86
104.5			-4.52			-4.52	-4.52	-8.84			-8.84	-8.84
105.5			-4.93	-4.74	-4.81	-4.83	-4.80	-8.80	-8.41	-9.09	-8.77	-8.90
106.5			-4.67	-4.66		-4.63	-4.60	-8.81	-9.28		-9.04	-9.15
107.5			-4.63	-4.54		-4.58	-4.58	-9.21	-9.10		-9.16	-9.12
108.5			-4.47	-4.64		-4.56	-4.62	-8.85	-9.08		-8.97	-9.05
109.5			-4.24	-4.57		-4.40	-4.54	-9.42	-8.85		-9.14	-8.90
110.5			-4.41	-4.49		-4.45	-4.46	-8.87	-8.97		-8.92	-8.94
111.5			-4.51	-4.64		-4.58	-4.60	-8.54	-8.94		-8.74	-8.83
112.5			-4.69	-4.78		-4.74	-4.76	-9.17	-9.12		-9.15	-9.13
113.5			-4.55	-4.60		-4.58	-4.58	-8.85	-8.83		-8.84	-8.84
114.5			-4.94	-4.63		-4.79	-4.66	-9.66	-9.00		-9.33	-9.07
115.5			-4.67	-5.02		-4.85	-4.82	-8.60	-9.05		-8.83	-8.91
116.5			-5.02	-5.15		-5.08	-5.11	-9.07	-9.01		-9.04	-9.03

which limits transfer of summer evaporative enrichment to bulk lake water  $\delta^{18}\text{O}$ . The influence of high (and isotopically heavy) precipitation events during summer is also dampened by the rapid throughflow of surface water. This summer bypass effect naturally counteracts the impact of both dry and wet summer conditions on the isotopic composition of the lake water and should serve to minimize changes in the offset between  $\delta^{18}\text{O}_L$  and  $\delta^{18}\text{O}_P$ . Consideration of hydrogen

isotope data from the lake water indicates that most of the  $^{18}\text{O}$  enrichment (ca. 0.75‰) is attributable to long-term steady state evaporation.

The summer variations only influence the epilimnion and are transferred to the bulk water body by the winter mixis. Therefore, the changes in  $\delta^{18}\text{O}$  of the hypolimnion are small compared to the seasonal variations of the epilimnion. During winter the input and its isotopic signal are distributed

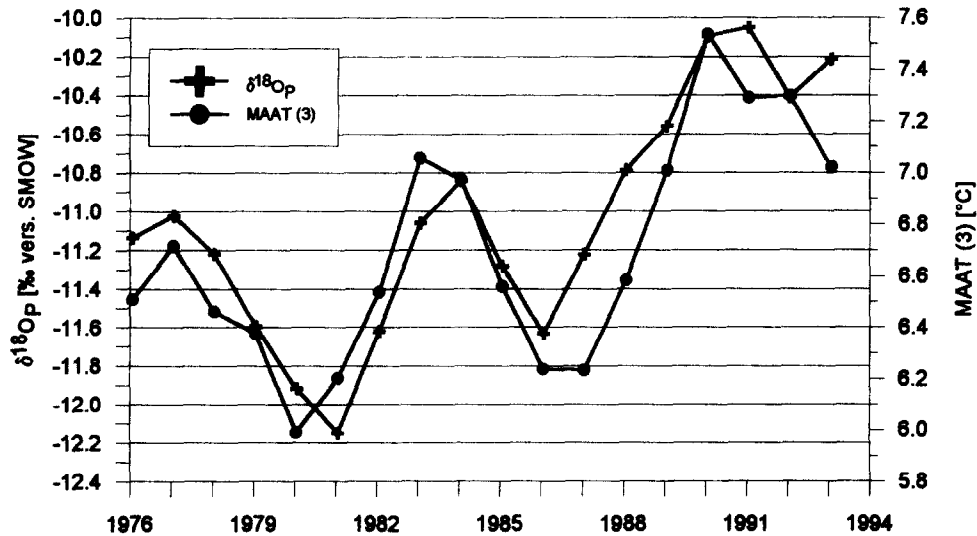


FIG. 3. Three-year-running means of  $\delta^{18}\text{O}_p$  and of mean annual air temperatures 1976–1993.

over the bulk water mass. During summer the hypolimnion remains rather constant. Deep water samples should, therefore, express the bulk yearly reaction of the lake to the last seasonal cycle. From 1990–1994,  $\delta^{18}\text{O}$  of the mixed lake showed an increase of 0.5‰ in accordance with the increase of MAAT and mean  $\delta^{18}\text{O}_p$  (Fig. 3) of the years before.

We used a simple two-box model to test the reaction of  $\delta^{18}\text{O}_L$  to climatic variations differing in amplitude and frequency. The model describes the response of  $\delta^{18}\text{O}_L$  to changes in  $\delta^{18}\text{O}_p$ , which in turn is derived from MAAT using an assumed linear relation.  $^{18}\text{O}$  of the input ( $\delta^{18}\text{O}_I$ ) is assigned to be a three-year running mean of  $\delta^{18}\text{O}_p$  weighted by the amount of precipitation. The combined isotope and mass balance of the lake is calculated separately for the summer season (April to September), when only the epilimnion is altered by  $\delta^{18}\text{O}_I = \delta^{18}\text{O}_p + 0.5\text{‰}$  and by evaporation, which is allowed to change relatively in inverse proportion to the relative change in precipitation. For the winter season the epilimnion and hypolimnion are allowed to mix and input changes influence the whole water column such that  $\delta^{18}\text{O}_I = \delta^{18}\text{O}_p - 0.5\text{‰}$  (see appendix for further details).

First, we tested the sensitivity of the model lake to theoretical climatic variations in the form of square waves of different frequencies, by comparing the resulting  $\delta^{18}\text{O}_L$ -MAAT relation with the input  $\delta^{18}\text{O}_p$ -MAAT relation. The response of the  $\delta^{18}\text{O}_L$ -MAAT relation decreases from close to one times the  $\delta^{18}\text{O}_p$ -MAAT gradient at 100 years to 0.85 at 12 y. This dampening of the response is caused by proportionally increasing times of incomplete response following the positive and negative shifts, biasing the resulting relation. For periods shorter than 12 y, the response relation declines more dramatically with period, because the lake never reaches a steady state, and hence the ultimate response to a shift is decreased.

We also tested the robustness of the resulting  $\delta^{18}\text{O}_L$ -MAAT relations by introducing precipitation amounts randomly covering a range two times larger than the limits observed between 1880 and 1980. Even this unrealistic sce-

nario does not significantly perturb the relations between  $\delta^{18}\text{O}_L$  and MAAT for the different frequencies. The model was also used to show the response of the lake system to an arbitrary air temperature development randomizing within 5 and 7.5°C, allowing hydrological variations over double long-term range. Even this irregular pattern produces a positive correlation between  $\delta^{18}\text{O}_L$  and MAAT, but the slope of the response relation is reduced to about half of the used  $\delta^{18}\text{O}_p$ -MAAT relation and frequencies below three year periods are suppressed.

A similar test can be undertaken using the temperature time-series from Hohenpeißenberg (see below and Fig. 8). Actual precipitation data were used for the time following 1880, for which records are available. For the period prior to this we simulated precipitation data by randomizing within the range observed from 1880–1994.

### 3.3. Reconstruction of $\delta^{18}\text{O}_L$ during the Last 300 Years

The oxygen isotope compositions of juvenile *Candona sp.* ( $\delta^{18}\text{O}_{C.s.}$ ) from sediment core AS Tmax 88 (Fig. 5) cover a range from  $-4.35\text{‰}$  to  $-5.35\text{‰}$ . The values are reproducible as shown by the small differences of replicate measurement from most of the samples. The highest values are found at 70 cm and 110 cm core depth, the lowest at 9 cm, at a short period around 19 cm, within a longer interval of mainly low values between 38 cm and 60 cm core depth, around 74 cm, and around 93 cm. Due to the limited water temperature variations at the core position, fluctuations in  $\delta^{18}\text{O}_{C.s.}$  are primarily controlled by the oxygen isotope composition of the hypolimnic water body during the time of the calcite formation, i.e., the time shortly after the molting of an individual animal. Studies of the population dynamics of *Candona levanderi* and *C. candida* in Ammersee and Starnberger See show that their ontogenic development is strongly related to the mixing of the lakes. Living larvae of the instars 5–8 of these species in deep lake sites below the thermocline were only found immediately after mixis reached the sites.

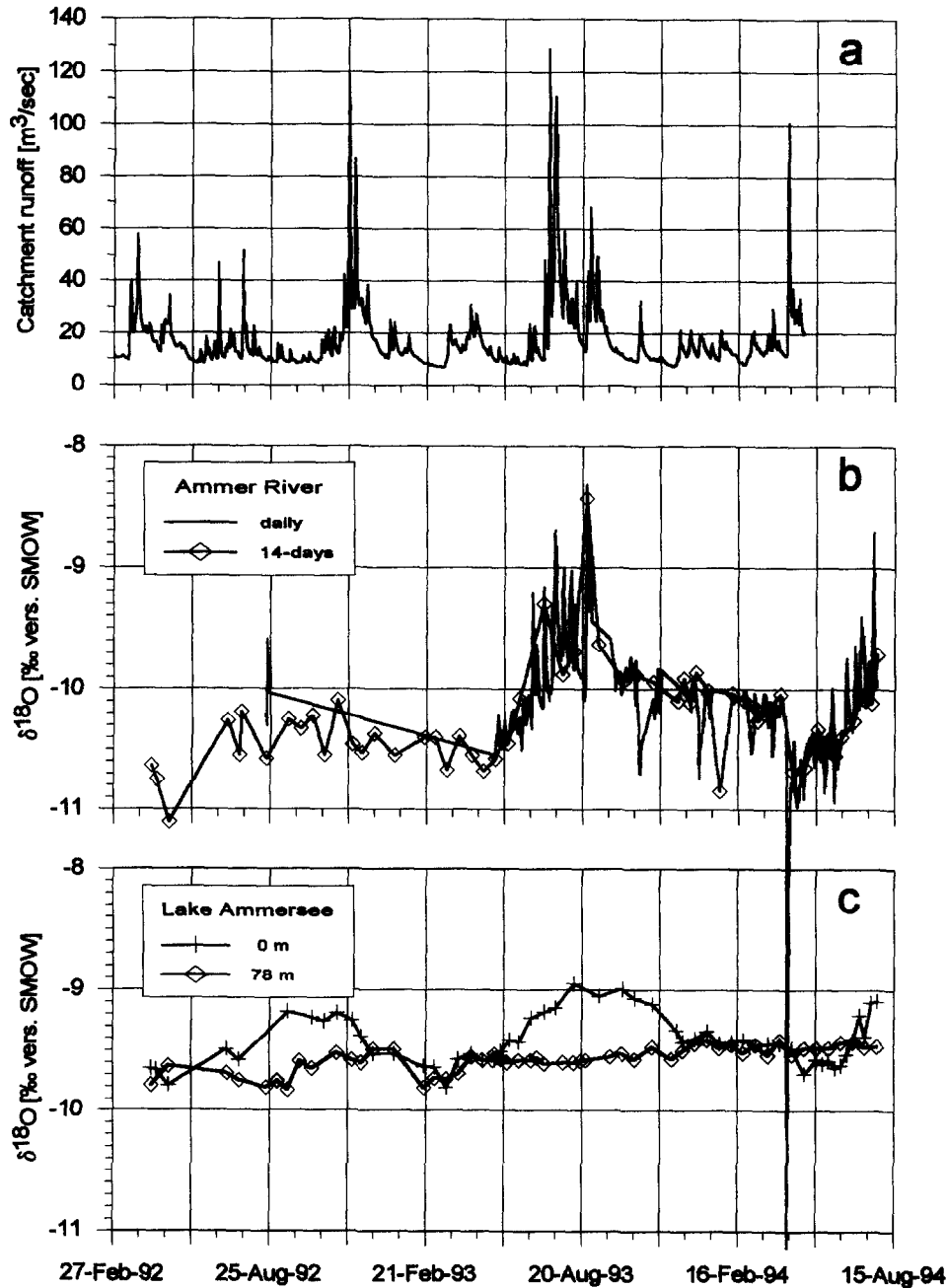


FIG. 4. (a) Mean daily runoff from spring 1992 to summer 1994. (b) stable oxygen isotope ratios of the main tributary of Lake Ammersee, Ammer ( $\delta^{18}\text{O}_{\text{Am}}$ ), (c)  $\delta^{18}\text{O}$  of the surface (crosses) and deep water (diamonds) of Lake Ammersee.

Bottom water temperatures during this time tend to decrease from an early mixing maximum of about  $4.5^{\circ}\text{C}$  to the winter minimum close to  $3.5^{\circ}\text{C}$ , with a mean around  $4^{\circ}\text{C}$ . We, therefore, can assume that the shells are built at  $4^{\circ}\text{C}$  and that  $\delta^{18}\text{O}_{\text{C.s.}}$  in AS Tmax 88 represents the oxygen isotope composition of the unstratified cold winter water body. Correcting for the vital offsets of  $2.3\text{‰}$  we can calculate  $\delta^{18}\text{O}_{\text{L}}$  of Lake Ammersee's hypolimnion for the time preserved in core AS Tmax 88 by

$$\delta^{18}\text{O}_{\text{L}} = \delta^{18}\text{O}_{\text{C.s.}} - 2.3\text{‰} - \Delta^{18}\text{O}_{(\text{Cc-H}_2\text{O}, 4^{\circ}\text{C})}, \quad (1)$$

where  $\Delta^{18}\text{O}_{(\text{Cc-H}_2\text{O}, 4^{\circ}\text{C})}$  represents the fractionation between calcite and water at  $4^{\circ}\text{C}$  according to Friedman and O'Neil (1977), including the conversion between the SMOW and PDB scales.

#### 4. DISCUSSION

According to the chronology of core AS Tmax 88, which is well established back to 1958, the rapid increase of  $\delta^{18}\text{O}_{\text{L}}$  from 18–16 cm must be correlated to the increase of MAAT prior to 1950. The low values of  $\delta^{18}\text{O}_{\text{L}}$  from 20 cm to 18

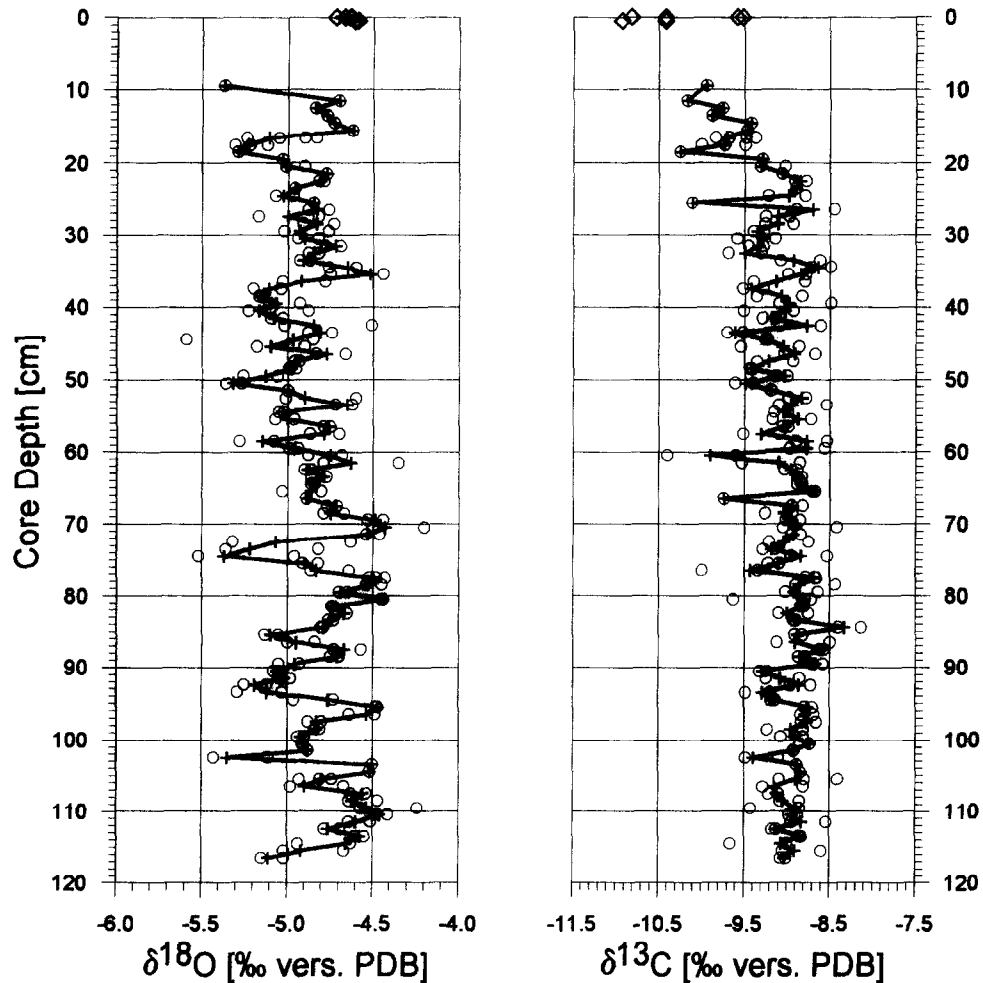


FIG. 5. Stable isotope values of *Candona* sp. (juveniles) vs. depth of core AS Tmax 88. Open circles show the individual measurements. The line connects the means of double or triple determinations weighted by the amount of shells in a subsample (crosses). Diamonds at 0 cm show  $\delta^{18}\text{O}$  and  $\delta^{13}\text{C}$  of *Candona* sp. (juveniles, instars 6 and 7) from winter 1992/1993 and winter 1993/1994.

cm preceding this increase match the cold years of 1941–1943. The rather constant climatic conditions of the time from 1900–1940 can be recognized in the  $\delta^{18}\text{O}_L$  with values around  $-4.9\text{‰}$  between 35 and 20 cm. Consequently, we can assume that the low values found below 38 cm should represent the time of low MAAT in the second part of the last century. The interval of high  $\delta^{18}\text{O}_{C.s.}$  between 72 and 68 cm should represent time around A.D. 1800, when MAAT was as high as the years 1990–1993. Using this correlation, the steep increase of  $\delta^{18}\text{O}_L$  from 75–72 cm matches the temperature increase from 1786–1796. The lowermost core interval from 110–70 cm should represent more or less the time from 1650–1800 with low temperatures similar to 1860–1890 in the middle part of the century and warm times comparable to 1800 and 1990 at the beginning of the 18th century.

We compared the  $\delta^{18}\text{O}$ -variations of core AS Tmax 88 (plotted on the timescale derived from layer counting, Fig. 6, upper graph) to running mean of MAAT from Hohenpeißenberg (Fig. 6, lower graph). Good agreement is appar-

ent between the records until about 1900 and from 1940 onwards. Between 1900 and 1940, all mean temperature excursions are visible in the  $\delta^{18}\text{O}_{C.s.}$ -record with more or less equivalent amplitudes and periods for the short-term variations, but with a lag of the measured MAAT of about 10 years compared to  $\delta^{18}\text{O}_{C.s.}$ . Given the obvious correlation of high-frequency variations and the uncertainties in layer counting and in the correlation between cores, it seems reasonable to slightly adjust the timescales to provide a better fit (Table 1). According to the mean accumulation rates, an error of 10 y would be about 2 cm on the depth scale. As mentioned above, such an error could be due to misinterpretations of light-dark couplets or a consequence of accumulation differences between the core AS Tmax 93 (used for counting) and core AS Tmax 88, or a combination of both.

A more subtle discontinuity between the records occurs around 1920, after which  $\delta^{18}\text{O}_{C.s.}$  appears to be shifted systematically downwards without an equivalent shift in MAAT. This shift can be quantified by plotting MAAT vs.  $\delta^{18}\text{O}_{C.s.}$  (Fig. 7). Pairs of  $\delta^{18}\text{O}_{C.s.}$  and MAAT minima and



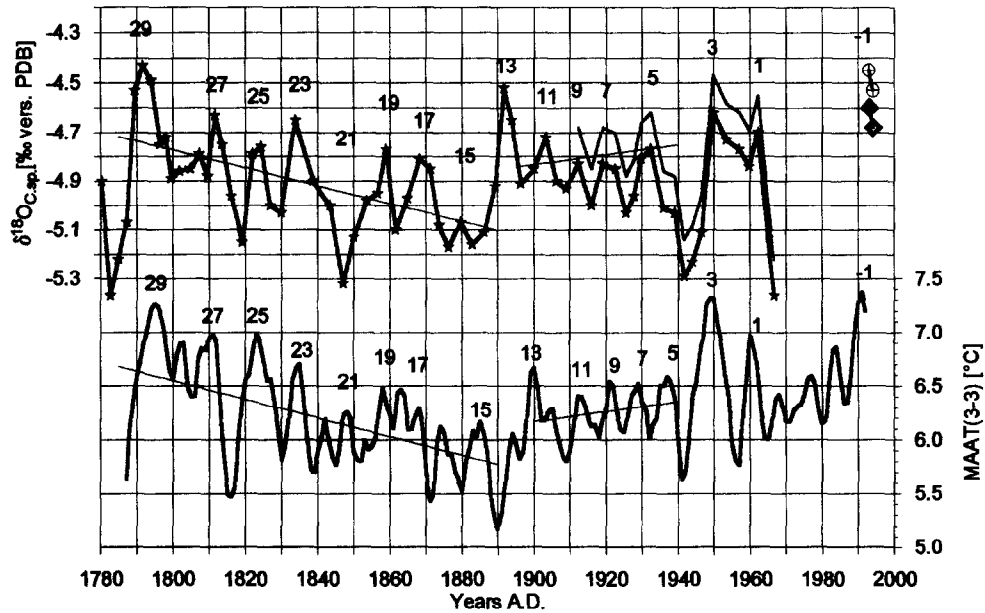


FIG. 6. Upper graph: Mean  $\delta^{18}\text{O}_{\text{C.s.}}$  of core AS TMax 88 (thicker line and stars) and  $\delta^{18}\text{O}$  from living *Candona* sp. in 1993 (diamonds). Lower graph: Two times three-year backward running means of MAAT from Hohenpeißenberg. To eliminate the effect of river regulation (see Fig. 5),  $\delta^{18}\text{O}_{\text{C.s.}}$  has to be corrected by  $+0.15\text{‰}$  for values younger than 1922 (upper graph, thinner line, encircled crosses for living material). The core chronology as inferred by the correlation with layer counted cores has to be corrected in the middle part of the core sequence (peaks 15 to 5) by about 10 years.

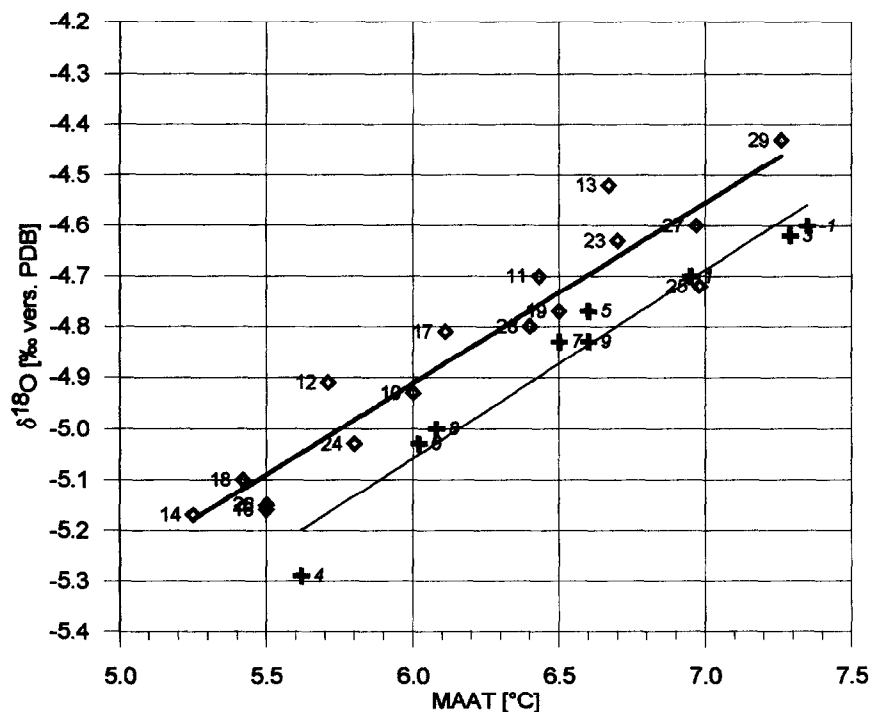


FIG. 7.  $\delta^{18}\text{O}_{\text{C.s.}}$  and 3-3-MAAT extrema of Fig. 6 (numbers as in Fig. 6). Pairs younger than 1922 (1 through 9, crosses) are shifted systematically by  $-0.15\text{‰}$  compared to the older values (11 through 29, diamonds) due to an increased bypass of summer precipitation following the Ammer river regulation. If these younger data are corrected by 0.15 the assemblage shows a linear relation with a slope of  $0.38\text{‰}/\text{K}$ , a correlation coefficient  $r^2$  of 0.91, and a standard deviation of  $0.07\text{‰}$  for  $\delta^{18}\text{O}_{\text{C.s.}}$ .

maxima, separated for the time before and after 1920 show a parallel offset by 0.15‰, indicating a singular shift of  $-0.15\text{‰}$  in  $\delta^{18}\text{O}_L$  around 1920 and persisting to the present. The timing of this shift corresponds with the modification of the runoff characteristics of the river Ammer noted above. Most probably, these changes caused a decrease in the  $\delta^{18}\text{O}_P$ - $\delta^{18}\text{O}_L$  separation by increasing the summer bypass effect.

Accounting for these two corrections provides the best fit for both the high-frequency signals expressed by the extrema and the low-frequency signals shown by decreasing  $\delta^{18}\text{O}$  and MAAT prior to 1900 and the slight increase in the early part of the 20th century.

Despite the consistency of trends in both  $\delta^{18}\text{O}_{C.s.}$  and MAAT and good agreements even in details, some of the extrema of the temperature history seem to be dampened (minimum 2 and peaks 15 and 25, for example) or exaggerated (peak 13, minima 4 and 20). These discrepancies may arise from the differences between the real timescale for the MAAT record and inferred timescale of the sedimentary record. The sample intervals are not equidistant on the timescale and include periods of varying duration depending on the accumulation rates. It is obvious that during times of higher accumulation, the  $\delta^{18}\text{O}_{C.s.}$ -value for a one-cm interval will be determined more by short-term conditions, whereas during times of lower accumulation the amplitudes of  $\delta^{18}\text{O}_{C.s.}$  can be considerably reduced due to the averaging over longer times. In cases where the arbitrary sample boundaries are in tune with the climatic changes,  $\delta^{18}\text{O}_{C.s.}$  will represent the ambient climatic conditions better than in cases where the sampled interval incidentally included times of strong gradients. This effect, in addition to the low pass filtering of the lake system, can lead to a scattering of the  $\delta^{18}\text{O}_{C.s.}$  compared to the true  $\delta^{18}\text{O}_L$  variations and will tend to decrease the significance and slope of the  $\delta^{18}\text{O}_L$ -MAAT relation ( $0.38\text{‰}/^\circ\text{C}$ , Fig. 7) inferred by  $\delta^{18}\text{O}_{C.s.}$ .

However,  $\delta^{18}\text{O}_L$  calculated with the simplified two-box model driven by the measured air temperatures (see above) show a striking similarity with  $\delta^{18}\text{O}_L$  as determined from the ostracod record corrected for the river regulation effect and the dating offsets (Fig. 8). We achieve the best fit of both  $\delta^{18}\text{O}_L$  records and the same slope of modelled and ostracod derived  $\delta^{18}\text{O}_L$ -MAAT relations ( $0.38\text{‰}/^\circ\text{C}$ ) by using a  $\delta^{18}\text{O}_P$ -MAAT of  $0.58\text{‰}/^\circ\text{C}$  as input. As expected, the similarity is higher for the time after 1880, where true precipitation data are available to drive the model, but even in the time before, where precipitation is assumed to be the average of the measured period, at least the long-term trend and the major high-frequency variations are similar. Of course, the successful modelling of the measured record is not a definite proof for the  $\delta^{18}\text{O}_P$ -MAAT relation of  $0.58\text{‰}/^\circ\text{C}$ , but it gives at least strong evidence that such a positive correlation also existed for the last 200 years and that the dampened lake response to the high-frequency MAAT oscillations should be the reason for the smaller gradient of the  $\delta^{18}\text{O}_L$ -MAAT relation compared to the  $\delta^{18}\text{O}_P$ -MAAT relation. The accuracy of the estimate of  $0.58\text{‰}/^\circ\text{C}$  for the slope of the  $\delta^{18}\text{O}_P$ -MAAT relation mainly depends on the quality of the correlation between  $\delta^{18}\text{O}_{C.s.}$  and MAAT (Fig. 7) and should be  $\pm 0.11\text{‰}/^\circ\text{C}$  ( $2\sigma$ ). The model itself could be improved by increasing the time resolution to monthly steps

and by incorporating evaporation and the resulting isotopic enrichment calculated using humidity and insolation data. We believe that this improvements will increase the accuracy of the model but would not significantly alter the main result, i.e., the temperature dependency of  $\delta^{18}\text{O}_L$  variations in Lake Ammersee and a probable  $\delta^{18}\text{O}_P$ -MAAT of about  $0.6\text{‰}/^\circ\text{C}$  for the last 200 years.

McKenzie and Hollander (1993) presented an oxygen-isotope record from varved sediments of Lake Greifensee (Switzerland) spanning the same time period, but measured on bulk carbonate. Their results are somewhat at variance to our record, showing a decrease of 3‰ for the last 100 y, which are explained by an increasing influence of westerly winds. The differences may be related to variations in the percentage of detrital carbonate, or the seasonality of carbonate precipitation or other factors that could be superimposed on the primary  $\delta^{18}\text{O}_P$ -signal in Greifensee (as discussed by McKenzie and Hollander, 1993), or to significant differences in the history of  $\delta^{18}\text{O}_P$  in Switzerland and southern Germany. Although detailed comparison of the Greifensee and Ammersee records is beyond the scope of the present article, it is clear that valuable opportunities exist to gain better understanding of the isotopic signals preserved in different archives, as well as to enhance knowledge about recent climate variability and change in the region.

## 5. CONCLUSIONS

The calibration of lake water isotopic variations derived from calcitic shells against an instrumental temperature record provides important information with respect to paleoclimatic reconstructions from similar archives. The most important one is that a  $\delta^{18}\text{O}_P$ -temperature relation of about  $0.6\text{‰}/^\circ\text{C}$  found by Rozanski et al. (1992) and (Rozanski et al., 1993) can apply to mid-Europe for the whole time of recorded instrumental air temperatures and, therefore, over a MAAT range exceeding the one of direct calibration by measuring both  $\delta^{18}\text{O}_P$  and temperatures. The temperature range covered by this indirect calibration is close to what should be expected for most parts of the Holocene, so the slope coefficient of  $0.58 \pm 0.11\text{‰}/^\circ\text{C}$  may probably apply to the whole Holocene.

However, the response of  $\delta^{18}\text{O}_L$  to the temperature controlled variations in  $\delta^{18}\text{O}_P$  will be characteristic for each lake and, therefore, must be evaluated by hydrological investigations for any lake used for paleoclimatic reconstructions. The response will not only depend on the lake's hydrology but also on the frequencies dominating the past temperatures variations. For long-term trends or big temperature shifts holding for longer times the lake response will be more complete and a relation closer to the local  $\delta^{18}\text{O}_P$ -MAAT relation will be valid, whereas short fluctuations of the order of the lake response time will be expressed in  $\delta^{18}\text{O}_L$  variations of amplitudes significantly smaller than expected from the  $\delta^{18}\text{O}_P$ -MAAT relation.

$\delta^{18}\text{O}_L$  of Lake Ammersee proved to be sensitive to mean air temperature variations with periods higher than 10 years and amplitudes larger than 0.3 Kelvin. Assuming no major changes of the hydrological geometry, we can assume the same sensitivity for at least the Holocene and probably for

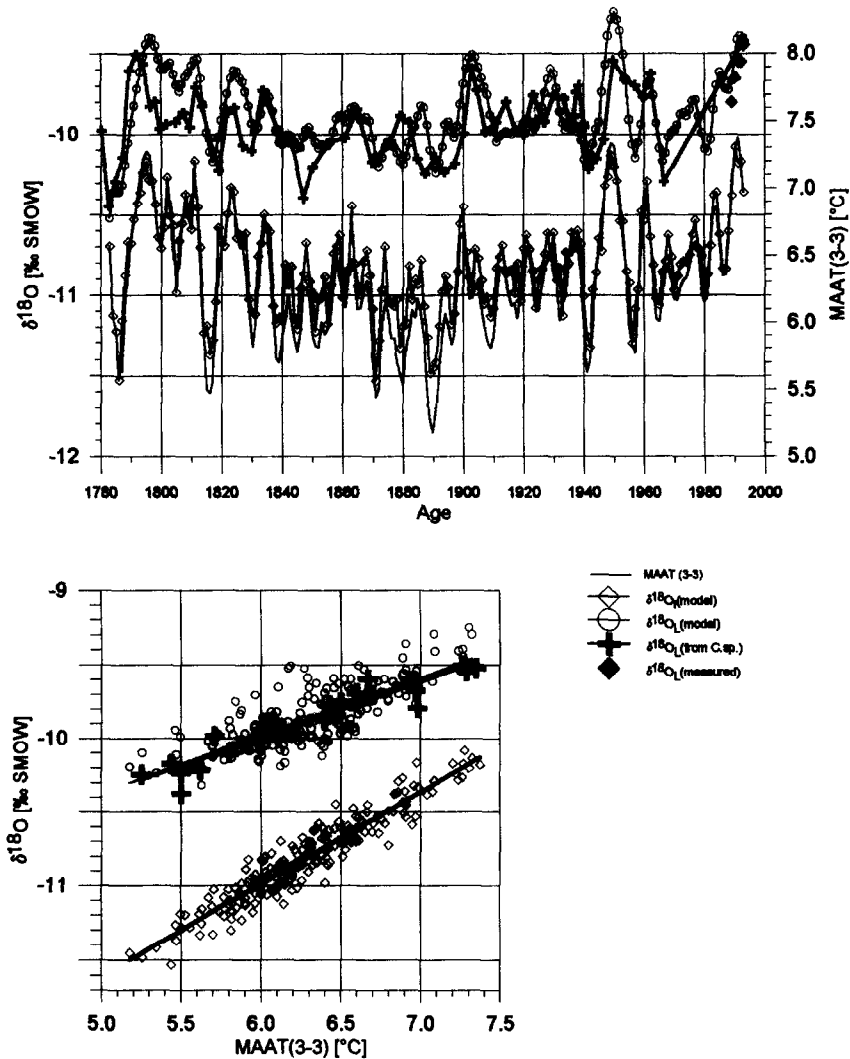


FIG. 8.  $\delta^{18}\text{O}$  of Lake Ammersee ( $\delta^{18}\text{O}_L$ ) as calculated from the measured ostracod  $\delta^{18}\text{O}$  record (crosses) compared to  $\delta^{18}\text{O}_L$  as predicted by a two-box isotope hydrology model (open circles) and to  $\delta^{18}\text{O}$  of the inflowing river ( $\delta^{18}\text{O}_r$ , diamonds), using  $\delta^{18}\text{O}_p = 0.58\text{‰} \cdot \text{MAAT} - 14.48\text{‰}$  as  $\delta^{18}\text{O}_p$ -MAAT relation. The upper graph shows the development over time. The lower graph compares the slope of the input relation (diamonds) to the slopes of the modelled (open circles) and of the measured (crosses)  $\delta^{18}\text{O}_L$ -MAAT relation. Ages of the lake record were adjusted by shifting within about ten years in the middle part of the record compared to Fig. 6.  $\delta^{18}\text{O}_L$  calculated from the ostracod record is corrected for the  $-0.15\text{‰}$  river regulation effect after 1922. Temperature variations dominate both the modelled and measured lake response. The slopes of the relation of both the modelled and the measured lake response to air temperatures are decreased compared to the  $\delta^{18}\text{O}_p$ -temperature relation due to the incomplete reactions of  $\delta^{18}\text{O}_L$  to the fast climatic changes.

the whole time since the deglaciation of the basin. First results of ostracod  $\delta^{18}\text{O}$ -studies from longer sediment cores indeed show climatic variations, which are consistent with pollen evidence and resemble both ice core isotope variations and marine paleotemperature reconstructions (Grafenstein et al., 1994). The results of this study show that it is promising to extend these paleoclimatic reconstructions for the last 14,000 years in order to get a high-resolution record of mid-European  $\delta^{18}\text{O}_p$ .

**Acknowledgments**—Meteorological data from Hohenpeißenberg were kindly provided by the German meteorological survey (Deutscher Wetterdienst), runoff data from River Ammer by the

Wasserwirtschaftsamt Weilheim. We thank H.-H. Cordt for running the Kiel mass spectrometer, and E. Kroemer and M. Herz for field assistance. The manuscript was highly improved by comments of and discussion with T. W. D. Edwards. The paper benefitted by the constructive and friendly reviews of Mrs. R. V. Krishnamurthy, J. Jouzel, and D. A. Hodell. The work was supported by the Bavarian government as part of BayFORKLIM as grant No. AII3.

*Editorial handling:* P. N. Froelich

## REFERENCES

Alefs J., Müller J., and Lenhart B. (1996) Die jährliche Änderungen der Diatomeenvergesellschaftung seit 1958 in einem warwenda-

- tierten Sedimentkern aus dem Ammersee (Oberbayern). *Limnologia* **26**, 39–48.
- Cuffey K. M., Clow G. D., Alley R. B., Stuiver M., Waddington E. D., and Saltus R. W. (1995) Large Arctic Temperature Change at the Wisconsin-Holocene Glacial Transition. *Science* **270**, 455–458.
- Dansgaard W. (1964) Stable isotopes in precipitation. *Tellus* **16**, 436–468.
- Deutscher Wetterdienst (1980–1994) Amtsblatt des deutschen Wetterdienstes: Monatlicher Wetterbericht.
- Friedman I. and O'Neil J. R. (1977) Compilation of Stable Isotope Fractionation Factors of Geochemical Interest. In *Data of Geochemistry* (ed. I. Friedman and J. R. O'Neil); *USGS Prof. Paper* 440-KK, KK1–KK12.
- von Grafenstein U., Erlenkeuser H., Kleinmann A., Müller J., and Trimbom P. (1994) High-frequency climatic oscillations as revealed by oxygen-isotope records of benthic organisms (Ammersee, southern Germany). *J. Paleolimnol.* **11**, 349–357.
- Grimminger H. (1982) *Verzeichnis der Bayerischen Seen*. Landesamt Wasserwirtschaft.
- Johnsen S. J. et al. (1992) Irregular glacial interstadials recorded in a new Greenland ice core. *Nature* **359**, 311–313.
- Johnsen S. J., Dahl-Jensen D., Dansgaard W., and Gundestrup N. (1995) Greenland palaeotemperatures derived from GRIP bore hole temperature and ice isotope profiles. *Tellus* **47B**, 624–629.
- Jouzel J., Koster R. D., Suozzo R. J., and Russell G. L. (1994) Stable water isotope behavior during the LGM: A GCM analysis. *J. Geophys. Res.* **99**, 25791–25801.
- McKenzie J. A. and Hollander D. J. (1993) Oxygen-Isotope record in recent carbonate sediments from Lake Greifen, Switzerland (1750–1986): Application of continental isotopic indicator for evaluation of changes in climate and atmospheric circulation patterns. In *Climate Change in Continental Isotopic Records* (ed. P. K. Swart et al.); *Geophys. Monogr.* **78**, 101–1110. AGU.
- Müller J., Sigl W., Michler G., and Sommerhoff G. (1977) Die Sedimentationsbedingungen im Ammersee—untersucht an Sedimentkernen aus dem Delta-, Profundal- und Litoralbereich. *Mittl. geographischen Gesellschaft München* **62**, 75–88.
- Rozanski K. (1985) Deuterium and Oxygen-18 in European groundwaters—Links to atmospheric circulation in the past. *Chem. Geol. Isotope Geosci. Sect.* **52**, 349–363.
- Rozanski K., Araguás-Araguás L., and Gonfanti R. (1992) Relation between long-term Trends of Oxygen-18 Isotope Composition of Precipitation and Climate. *Science* **258**, 981–985.
- Rozanski K., Araguás-Araguás L., and Gonfanti R. (1993) Isotopic patterns in modern global precipitation. In *Climate Change in Continental Isotopic Records* (ed. P. K. Swart et al.) *Geophys. Monogr.* **78**, 1–36. AGU.
- Stute M. (1989) Edelgase in Grundwasser—Bestimmung von Paläotemperaturen und Untersuchung der Dynamik von Grundwasserfließsystemen, unpublished thesis, Univ. Heidelberg.
- Schönwiese C.-D. (1987) Moving spectral analysis and some applications on long air temperature series. *J. Climate Appl. Meteorol.* **26**, 1723–1730.

## APPENDIX

The model describes the reaction of  $\delta^{18}\text{O}_L$  to changes in air temperatures assuming a linear relation between  $\delta^{18}\text{O}_p$  and mean annual air temperature. The isotopic composition of the input of a year  $\delta^{18}\text{O}_{1(i)}$  is the precipitation weighted mean of the last three years

$$\delta^{18}\text{O}_{1(i)} = \Sigma(a * \text{MAAT}_{(j)} + b) * p_{(j)} / \Sigma p_{(j)}$$

(for  $j = (i - 2)$  to  $(i)$ ),

where  $p_{(i)}$  is the ratio of the yearly precipitation  $P_{(i)}$  to the long-term yearly average of precipitation  $P$ . The isotopic composition of the epilimnion  $\delta^{18}\text{O}_{\text{Epi}(i)}$  for a summer half year is calculated using:

$$\delta^{18}\text{O}_{\text{Epi}(i)} = ((\delta^{18}\text{O}_{1(i)} + 0.5\text{‰}) * I / V_{\text{Epi}} * p_{(i)} * s_{(i)}) + (\delta^{18}\text{O}_{L(i-1)} * (1 - (I / V_{\text{Epi}} * p_{(i)} * s_{(i)}))) - ((\delta^{18}\text{O}_{L(i-1)} - \epsilon) * E / V_{\text{Epi}} / p_{(i)} / s_{(i)}),$$

where  $\delta^{18}\text{O}_{L(i-1)}$  is the isotope value calculated for the winter of the last year,  $I$  the long-term mean of the input,  $V_{\text{Epi}}$  the volume of the epilimnion,  $s_{(i)}$  the relative seasonality of precipitation ( $s_{(i)} = (P_{S(i)} / P_{(i)}) / (P_S / P)$ ),  $E$  the long-term mean of evaporation, and  $\epsilon$  the difference between  $\delta^{18}\text{O}_L$  and the evaporated moisture (which was assumed to be constantly 10‰).

The isotopic composition of the mixed winter water body  $\delta^{18}\text{O}_{L(i)}$  is produced by mixing summer epilimnion and the hypolimnion (showing the isotopic composition of the last winter), and by adding winter input:

$$\delta^{18}\text{O}_{L(i)} = ((\delta^{18}\text{O}_{L(i-1)} * V_{\text{Hyp}} / V + \delta^{18}\text{O}_{\text{Epi}(i)} * V_{\text{Epi}} / V) * (1 - (I / V * p_{(i)} * (1 - s_{(i)}))) + ((\delta^{18}\text{O}_{1(i)} - 0.5\text{‰}) * I / V * p_{(i)} * (1 - s_{(i)})).$$